URTeC: 2902624

Hydraulic Fractures in Core From Stimulated Reservoirs: Core Fracture Description of HFTS Slant Core, Midland Basin, West Texas

Julia F.W. Gale*, Sara J. Elliott, Stephen E. Laubach
Bureau of Economic Geology, The University of Texas at Austin, Austin, TX, United States.

Abstract

Objectives and Scope: The geometry and extent of the hydraulic-fracture network produced during well stimulation are generally not well known. Indirect methods such as microseismic monitoring may provide information about the network, but they are not definitive. The Hydraulic Fracture Test Site (HFTS) project was designed to recover core from a stimulated volume, thus providing direct information about hydraulic fractures. Here we present methods and some results from a fracture description of the HFTS slant well cores.
Methods: The 4-inch-diameter cores were contained within an aluminum tube and were examined prior to slabbing. We developed criteria for distinguishing between hydraulic, natural, drilling-induced, and core-handling fractures by examining the orientation and surface features of all fractures, making use of a CT scan of the core.
Results: More than 700 fractures total were found in 600 ft of core, including hydraulic fractures, two sets of calcite-sealed natural fractures, and drilling-induced and core-handling fractures. Hydraulic fractures were found to be most abundant in the section of core closest to the stimulated wells.
Significance: Benefits from an experiment of this type are: (1) Hydraulic fractures are observed directly, allowing fracture density and spatial distribution to be quantified. (2) Twist hackles on hydraulic-fracture surfaces may provide information about the direction of fracture propagation. (3) The degree to which natural, sealed fractures have been reactivated may be assessed. (4) Proppant distribution in the fractures can be examined. (5) Details of the observed hydraulic-fracture network can be used to verify, or provide input data for, models of hydraulic-fracture growth and proppant distribution. (6) Findings can provide ground truth for indirect diagnostic techniques such as microseismic monitoring. (7) Fractures in core and image log in the same well can be compared, and findings used to help calibrate other horizontal well image logs.

Introduction

Knowledge of the extent and geometry of hydraulic-fracture (HF) networks in unconventional reservoirs is generally limited. Operators instead rely on indirect observation of HF growth through tracking of microseismic activity (e.g., Fisher and Warpinski, 2012), and replication of HF growth and interaction with weak planes in geomechanical experiments (e.g., Lee et al., 2015). Whereas these techniques provide many useful insights, verification of results by direct observation of hydraulic fractures is needed, and the best method of achieving this verification is to take core through intervals that have been hydraulically fractured. Previous studies adopting this method have examined HFs in tight-gas sandstones, including Warpinski et al. (1993) and Branagan et al. (1996) at the DOE MultiWell site in Colorado and Fast et al. (1994) in Lost Hills field, California. Raterman et al. (2017) reported a direct-sampling experiment in the Eagle Ford Formation, but in that case natural fractures were rare. The Hydraulic Fracture Test Site (HFTS) project described here acquired six cores comprising four continuous cores in the Upper Wolfcamp and two continuous cores in the Middle Wolfcamp from the Midland Basin, West Texas. In this case, calcite-filled natural fractures are abundant. Courtier et al. (2018) provide background on the wider project, whereas this paper

presents a qualitative description of fractures in the six cores from the slant well. We characterize natural, drilling-induced, and hydraulic fractures in the slant core, and comment on reactivation of sealed natural fractures and bedding planes. Material including proppant in open fractures was collected and analyzed at the same time as the fracture description, and it is presented in a separate paper (Elliott et al., 2018).

Slant Core Methods: Acquisition, Handling, and Preparation for Analysis

Locations of cores along the well were selected to optimize chances of capturing hydraulic fractures from two nearby stimulated wells (6U and 6M). Approximately 600 ft of core was recovered: about 400 ft in four continuous cores from the Upper Wolfcamp and about 200 ft in two continuous cores from the Middle Wolfcamp. The cores were encased in aluminum tubing to minimize breakup along fractures. CT scans of the core were made at CoreLabs prior to core observation, and the zero datum for the CT scan was marked on the core ends. CT scans proved invaluable in mapping fractures in the core, with clear imagery of lithology changes, bedding, sealed natural fractures, and open fractures. The scans provided a ready 3D inventory of fractures for documentation purposes, and any fractures caused by core handling after the CT scans were done, or that were the result of core desiccation, could be identified as such by comparison of the CT scan with our direct observation. A further benefit of having the CT scan ahead of removing the core from the aluminum tubes was that we were able to anticipate the amount of fracturing and likely fragility of each 3-ft section. This knowledge was used to test three methods of removing core from the tube for observation, while preserving fracture features, and to decide whether to slab the core.

Method 1: the aluminum tube only was cut in a "clam shell," with a 50:50 cut subparallel to bedding (Fig. 1). Fractures were easily examined after the drilling mud had been scraped off. Core pieces could be taken out and replaced, and the aluminum tube could be replaced once examination was complete. Damage to core was minimized using this method. Once the analysis was done, the whole assembly (core and tube) was put back together and secured with shrink wrap for storage. This method was found to be superior.

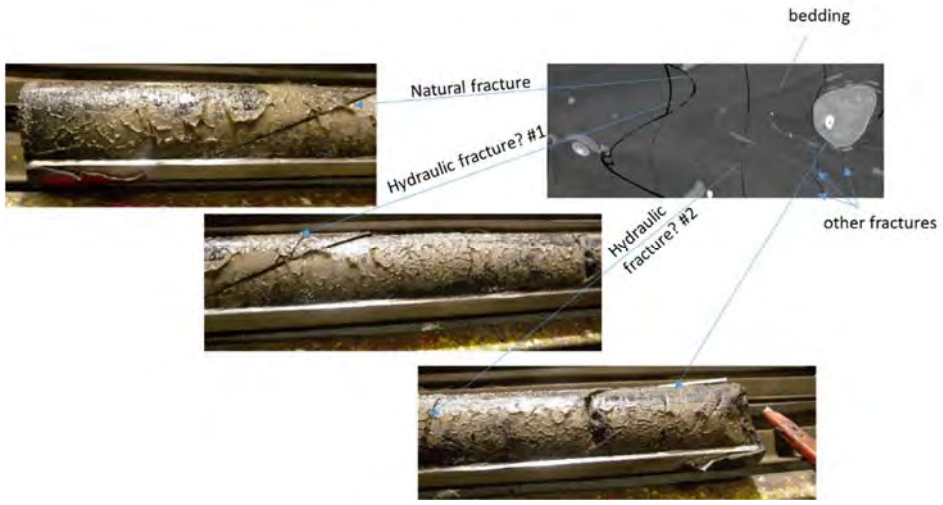

Figure 1. Core left whole while aluminum tube is bisected and opened to reveal core ("clam-shell" method). Example test on section, where core has several fractures. Top right = CT scan for this 3-ft section.

Method 2: two 2-ft sections were stabilized with red-stained epoxy prior to slabbing (Fig. 2). Sections that were epoxied and then slabbed subparallel to bedding were stabilized successfully, although the fracture surfaces are no longer visible (Fig. 2a). Whereas this technique prevents further breakup of core, it is the least-desirable option because inspection of fracture surfaces is essential for determining fracture origin. Also, because introduction of epoxy widened some of the fractures considerably (up to 1 cm), the geometry now observed is not the true, original, fracture geometry (Fig. 2b). No further sections were epoxied. Method 3: core was slabbed in the sleeve with no stabilization (Fig. 3a). The CT scan (Fig. 3b) showed that this short section had several fractures in it. The pieces of core, however, could not easily be taken out of the halved tube and had to be turned out on the bench for observation

of fracture faces. This activity resulted in new breaks being created in the core (Fig. 3c), and it was decided that slabbing, even with the core in the tube, was too damaging and should not be done prior to fracture description.

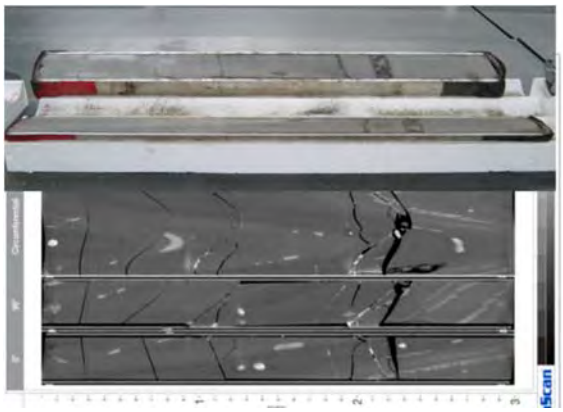

Figure 2. (a) CT scan and photograph of slabbed core. Core section has multiple breaks and was treated with red epoxy prior to slabbing. (b) In places, force of introducing epoxy (red material) had widened existing fractures from original width of 1–2 mm to ~1 cm.

Systematic Description Methodology

The systematic description of fractures includes information on depth, orientation, aperture and fill of natural fractures, length and height, morphology and surface features, presence of proppant pack, information on faults, and an assessment of fracture origin, together with a measure of certainty of interpretation. This paper summarizes descriptive methods and provides some qualitative results. A quantitative paper will follow.

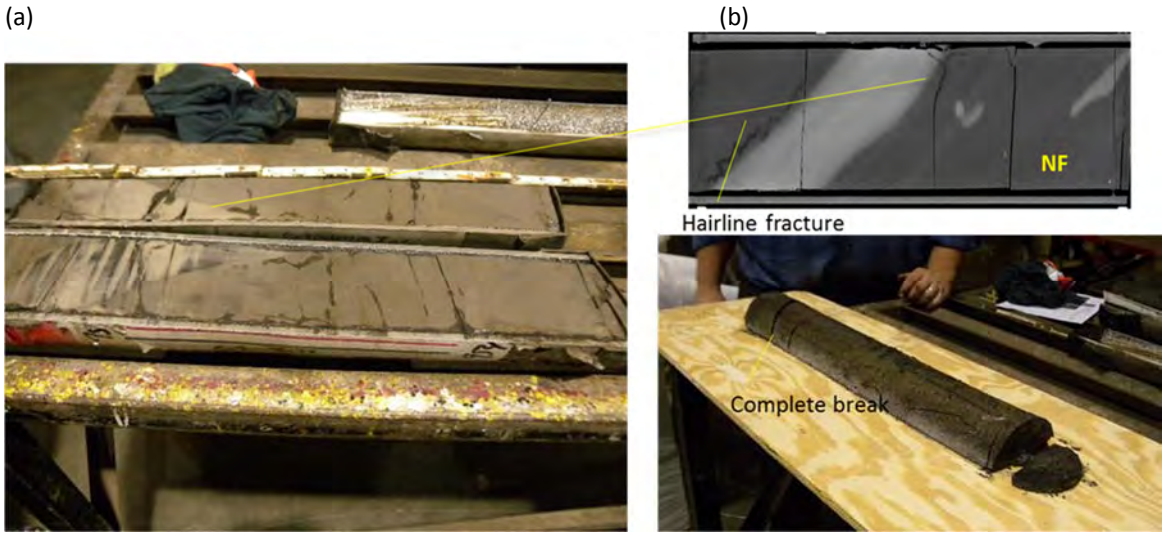

Figure 3. (a) Slabbed section inside aluminum tube. Fracture faces cannot be observed without removing core from tube. (b) Slice through CT scan of interval. Pale layer is carbonate and can be seen in core in a. (c) Core has been removed from tube and inverted on bench. Act of slabbing and removing core from tube generated new complete break, beginnings of which are visible as partial hairline fracture on CT scan.

Depth and Number

Fracture depths were reported by measured depth (MD) at the uphole limit of the fracture. Each fracture is uniquely identifiable by a 3-ft core section and a fracture number.

Orientation

Fracture orientations were measured by Busetti and Farrell (unpublished HFTS report) and integrated with our fracture descriptions. We performed a qualitative check that orientations were consistent with our interpretation, using the CT scan to aid in identification and description. Bedding is clear in most sections owing to variation in carbonate content of adjacent beds (Figs. 1–3). In a few locations, the bedding dip azimuth and core axis are close to parallel because of changes in bedding orientation. Bedding undulates around concretions as well.

Aperture and fill

Fracture width (kinematic aperture) is the wall-to-wall distance measured normal to the fracture, including mineral fill and any opening. For intact fractures in the slant core that are mostly less than 1 mm wide, we used a ruler (comparator) with calibrated, logarithmically graduated widths marked for comparison with fracture kinematic aperture (Ortega et al., 2006). Measurements were thus binned according to the marked widths. For parted fractures, thickness of cement on walls was measured and reported as a minimum aperture. If filled, mineral cement type was identified and completeness of fill noted as a percentage.

Length and height

Because most fractures continue beyond core boundaries, length and height data cannot be obtained. If a fracture terminates within the core, however, the nature of the termination can be interpreted—for example, a gradual taper to the tip or an abrupt termination at a lithology change, a bedding plane, or another fracture. For fractures completely contained within the core, the length or height was recorded.

Morphology and surface features

Fractures may be planar, curviplanar, or irregular. Surface markings include slickensides, plumose structure, twist hackles, and arrest lines. Some fractures have remarkably smooth faces; others are rough and irregular. We used this difference to distinguish between fractures that formed under large confining stress in the subsurface (HFs or drilling-induced fractures) from those formed during core retrieval or handling.

Fracture origin

Each fracture was described and classified, together with an uncertainty indicator—sure, probable, and best guess. The *sure* category was reserved for natural fractures in which cement could be seen or for hydraulic fractures in which a thick proppant pack or proppant patches were present. Otherwise, most hydraulic fractures were classified as *probable*, given the uncertainty as to whether they could be drilling induced. *Best guess*, the least-certain classification, was made on the basis of a combination of features such as orientation, morphology, and surface features.

Results: Fracture Description and Criteria for Fracture Classification

Each of the fracture types are described and we outline criteria used to differentiate them, as well as to identify natural-fracture reactivation. The different fracture types are presented in chronological order of formation: natural, drilling induced, hydraulic, and core handling.

Natural fractures

Two main sets of natural opening-mode fractures filled with calcite cement are present: Set 1 trends broadly NE–SW (Figs. 4a, 5a), and Set 2 trends WNW–ESE (Figs. 4b, 5b), both with steep dips. These natural fractures are identified primarily on the basis of calcite mineral fill. Fractures may be fully sealed and intact, partly sealed and intact (with original fracture porosity), or parted (Fig. 4a). In the latter case, cement can be seen on the fracture wall(s). This cement can be subtle and present as a patchy veneer on one or both surfaces. In some fractures, positive cement identification is challenging—dried drilling mud can also resemble a pale cement veneer. The mud reacts with dilute HCl (owing to carbonate entrained in the mud) so that an acid-drop test cannot be used to identify cement. A small chip from such a fracture surface at the end of one core was imaged and examined using SEM-based EDS. The material on the surface proved to be dried drilling mud. When positive identification of cement is not possible, orientation is a useful indicator of fracture origin, although it is not definitive by itself. In two locations Set 1 natural fractures have euhedral calcite cement on their surfaces, indicating they were open in the subsurface (Fig. 4c). We did not measure the kinematic aperture because these fractures are now parted, but we estimated them to have been more than 1 mm wide.

The natural, calcite-filled fractures in this well are typical of fractures in shale, occurring as narrow, composite groups typically less than 1 mm wide (c.f. those described by Gale et al., 2014, and references therein). The smallest are only a few centimeters in length and height, and the largest are perhaps 1 m or so long and high (but continue out of the core). Some are bed bound. Occurrences of other natural-fracture types are minor, including those internal to concretions and those related to deformation around concretions (Fig. 6).

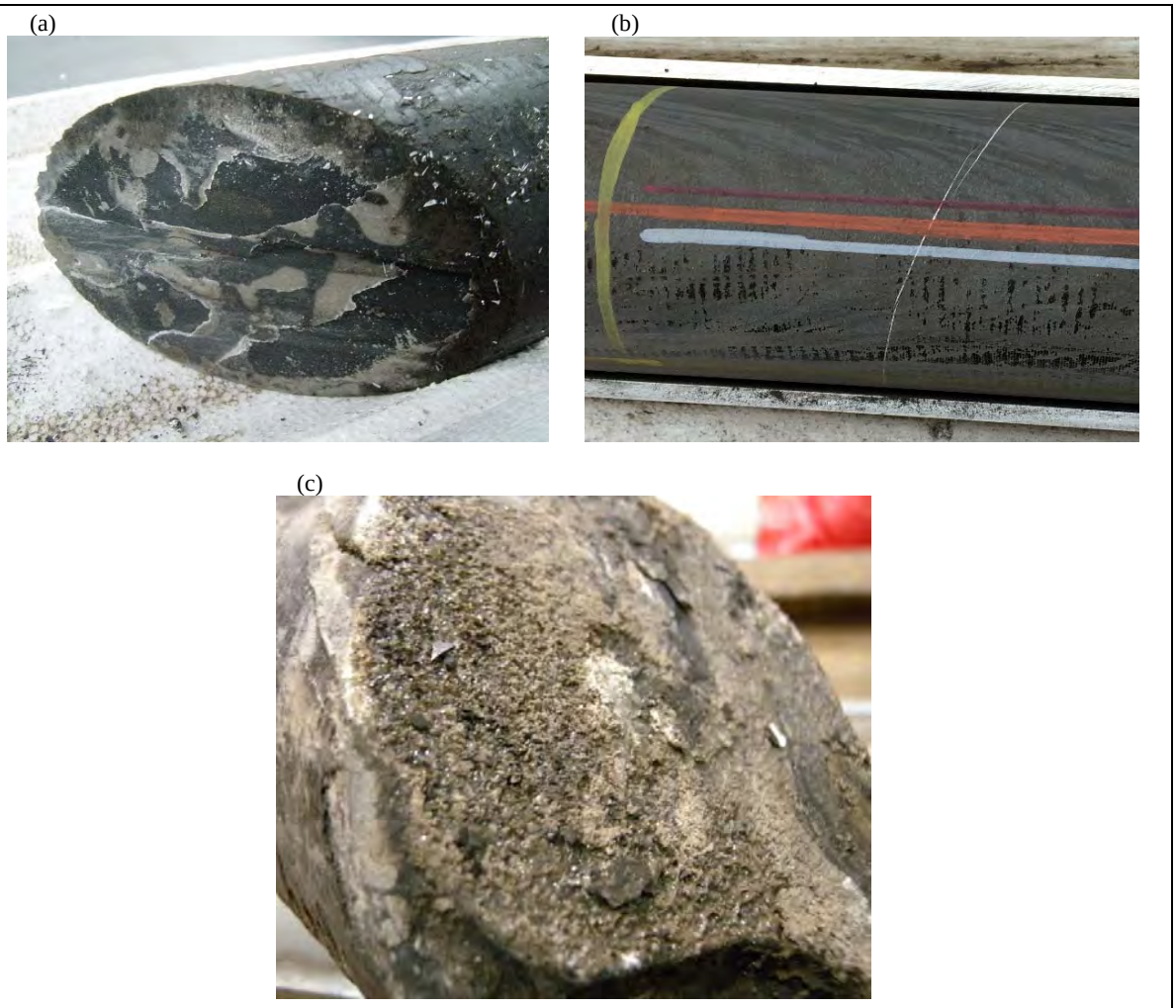

Figure 4. Natural fractures in the slant core. (a) Parted, Set 1 fracture with patchy calcite on fracture face. (b) Intact, Set 2 composite fracture; of the three segments, the middle segment is offset uphole from the other two by a few millimeters. Slight deviation of fracture path at tips indicates stresses ahead of tips were modified by presence of approaching neighbor. (c) Euhedral calcite crystals on Set 1 fracture face indicating fracture was open in subsurface.

Natural, bedding-parallel fractures are uncommon, occurring only around a few concretions, and we did not observe any “beef” (Cobbold et al., 2013). Core orientation and roughness of the outer surface, however, are not optimal for seeing narrow (<1 mm wide), bed-parallel fractures. Also, such fractures are challenging to distinguish from carbonate laminae on the CT scan. A few concretions have fractures on both margins with both calcite and pyrite fill, and there are also a few examples of pyrite-filled fractures internal to concretions. Other fractures in different orientations, filled with calcite and pyrite and having width:length aspect ratios that are generally greater than those for Set 1 and Set 2 fractures, are present in a few locations, mostly close to faults.

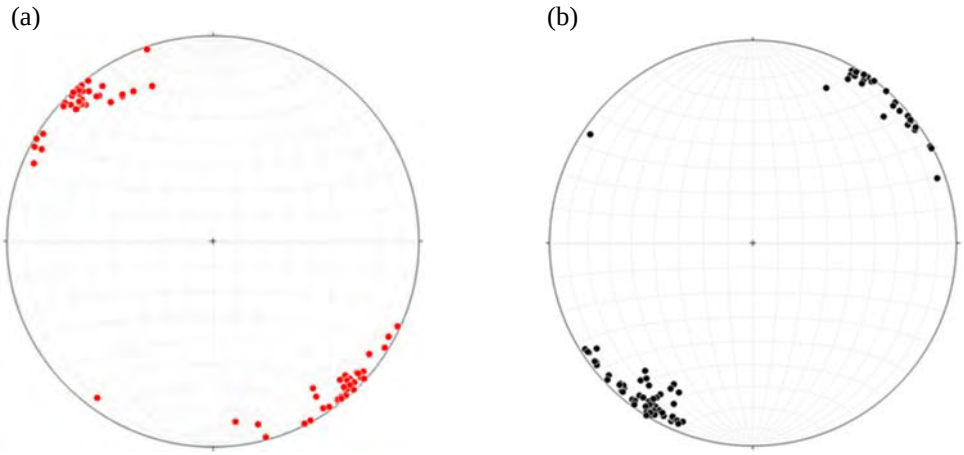

Figure 5. Lower-hemisphere stereograms of poles to calcite-filled natural fractures. (a) Set 1. (b) Set 2. Data from Busetti and Farrell's analysis.

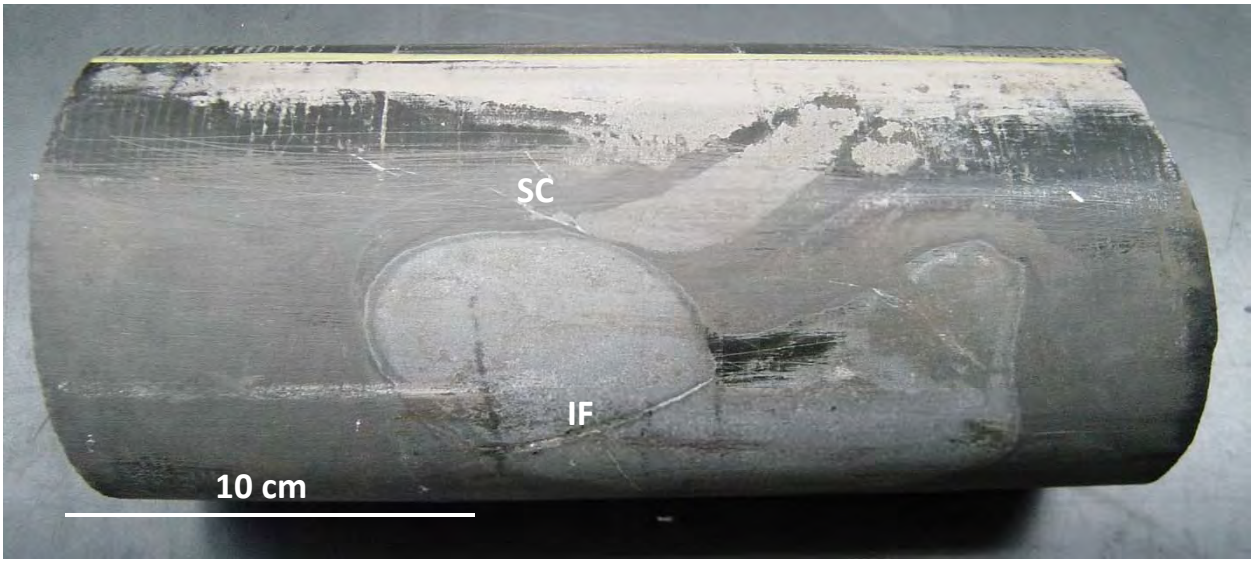

Figure 6. Calcite-filled fractures associated with concretions. Some fractures are internal to concretions stopping at boundaries (IF). Others develop in shale surrounding concretions (SC), most likely as result of strain localization around concretion.

Two types of fault occur: early, soft-sediment deformation faults (Fig. 7a) and later, moderately dipping faults with oblique slip, indicated by slickensides on the fault planes (Fig. 7a–c). In one fault oriented 292.5°/57.4° NE, slickensides suggest normal and dextral components of oblique slip. Some have a small amount of calcite cement.

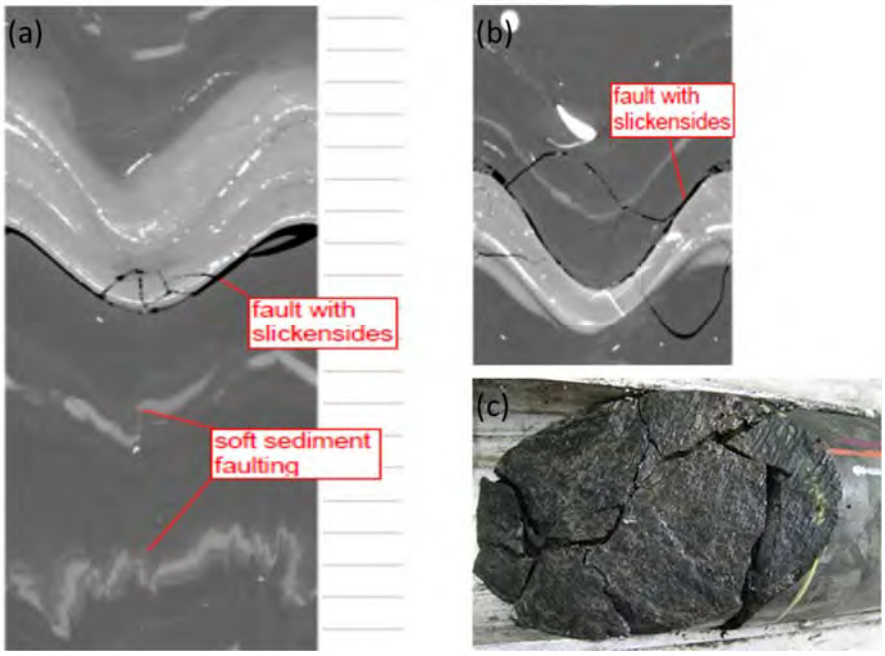

Figure 7. Faults in slant core. (a) CT scan of faulting and soft-sediment deformation. (b) CT scan of fault in (c), which has oblique slickensides.

Hydraulic fractures

A large number of barren, core-normal fractures are present, broadly trending E–W (Fig. 8), which is subparallel to S_{Hmax} in this part of the Midland Basin (Lund Snee and Zoback, 2016). Hydraulic fractures, present possibly as large planes of varying complexity, have been intersected in a singular location by core. We therefore see only a small snapshot of each fracture. Features on the fracture surfaces, such as twist hackles and plumose markings, developed at the time of fracturing and are not related to the drilling process; they do not originate near the core margin and are not core symmetric. A stereogram plotted for poles to measurable hydraulic fractures reveals an approximately 40° spread of dip azimuth, which may reflect local stress variations or branching geometries (Fig. 8).

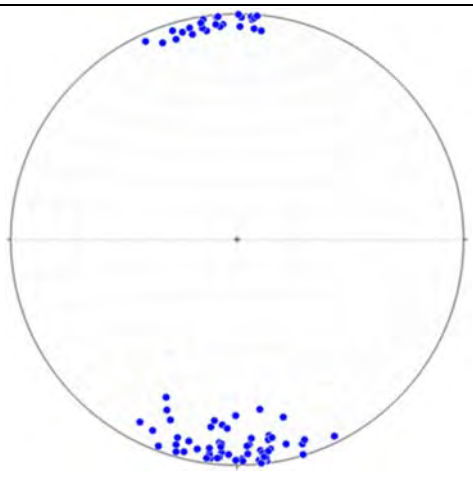

Figure 8. Lower-hemisphere stereogram of poles to hydraulic fractures. Data from Busetti and Farrell analysis.

Occurrence of hydraulic fractures in the cores is heterogeneous, with both clusters and interval with no fractures. Many are single planar breaks with smooth surfaces, and some have a stepped geometry (Fig. 9). In other cases, two or more breaks are closely spaced, suggesting bifurcation. Clusters of two to four core-normal fractures in the space of a few centimeters are common and may be multiple hydraulic-fracture strands (Fig. 10). In rare cases, bifurcation is captured in the core and can be used to infer the direction of hydraulic-fracture growth.

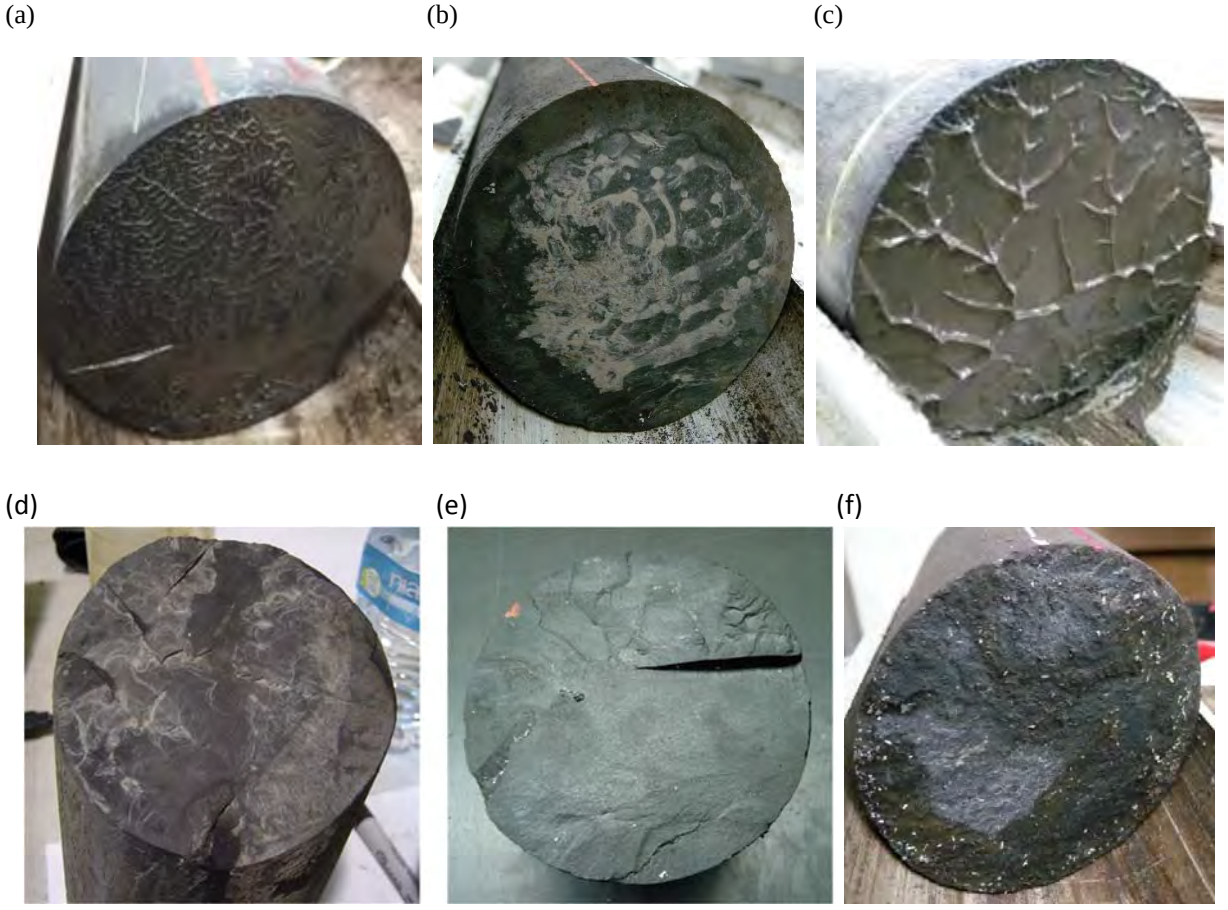

Figure 9. Surface character of hydraulic fractures. (a) Smooth face with one step and wet drilling mud. (b) Smooth, planar, featureless face with dried mud in center and wet mud around perimeter. (c) Smooth, planar surface with thick drilling mud and no obvious sand. Note this fracture is just 3.3 ft below the fracture complex that has a thick proppant sand pack (Fig. 13). (d) Stepped, somewhat irregular face. (e) Partly smooth face with one large step. (f) Somewhat irregular face in coarser carbonate layer.

In addition to bifurcation, surface markings such as twist hackles may be used to determine local propagation direction of the fracture (Fig. 11). Twist hackles initiating at mechanical-layer changes are orthogonal to the layer and gradually taper out away from the point of initiation. These may be used to indicate the local direction of hydraulic-fracture propagation. In some cases, determining wider-scale lateral propagation on the basis of asymmetry of twist-hackle steps may be possible. Multiple examples of twist hackles occur in the slant core—some suggesting local upward propagation, others downward, some large-scale eastward propagation, and some westward.

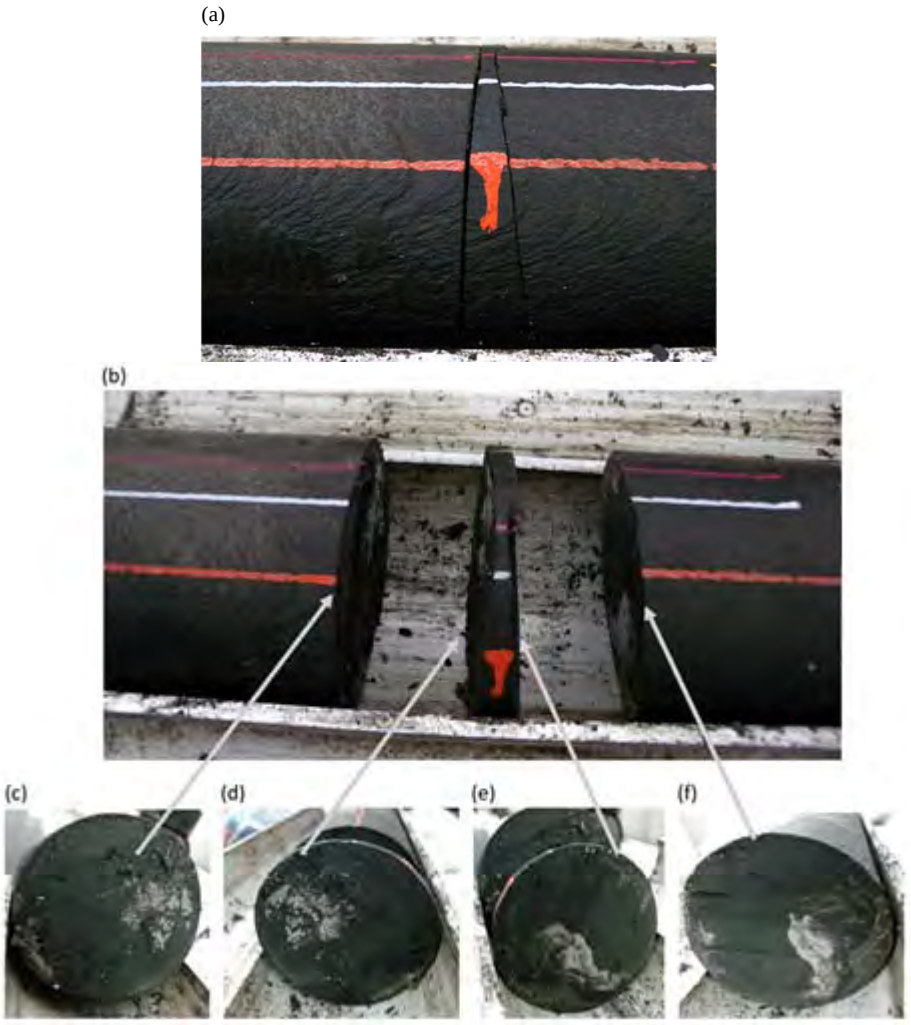

Figure 10. (a) Two, closely spaced but non-parallel hydraulic fractures indicating bifurcation and propagation to the west (orange mark = core top). (b) Core pieces pulled apart. (d–f) Fracture faces in b.

Some twist hackles have apparently anomalous geometries, however, in that the inferred propagation direction is not consistent with the relative positions of the nearest stimulation well and the slant well. In one example (Fig. 12), twist hackles initiate off bedding and suggest local downward propagation. Twist-hackle asymmetry suggests that overall propagation is to the east, but the 6U well is below and to the east of the slant core at this location, and hydraulic fractures would therefore be expected to grow up and to the west.

Hydraulic fractures with proppant pack

Hydraulic fractures contain a sand (proppant) pack in three locations, all of which lie within a more intensely fractured interval in the Upper Wolfcamp (Figs. 13–15). In one example sand occurs as patches on a fracture face that is part of a HF doublet (Fig. 13). Notably no drilling mud is present, indicating that the sand was in place prior to drilling. The thickest sand pack occurs at a location where the HF is branched and the pack is present in each strand (Fig. 14). The total complex is approximately 1 cm thick. The third sand pack location is at a concretion (Fig. 15). Where HFs encounter concretions, fractures become complex, and the concretions are shattered. The sand is visible in the fracture at the uphole end but can also be seen in some of the other breaks. A piece of the sand pack appears to have been pushed out of the fracture (Fig. 15a)—it was sampled and the remainder left intact. The CT scan shows a bright signal in the fractures and in the concretion, which is likely pyrite (Fig. 15b). The dark-gray signal of proppant noted in Figure 14a is not apparent, possibly being obscured by the pyrite.

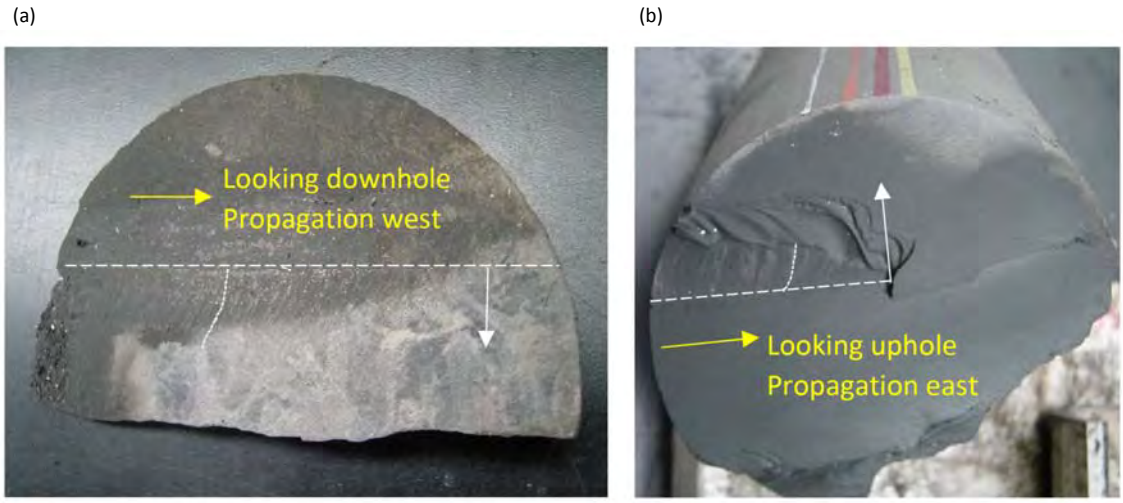

Figure 11. Examples of twist hackles (TH). Dashed line = initiation plane. Local direction of growth is normal to that line (white arrow). Overall fracture propagation direction given by yellow arrow. (a) Upper Wolfcamp example; view downhole. TH initiate at pyrite layer. Propagation down and west. (b) Middle Wolfcamp example; view uphole. TH initiate at bedding plane. Propagation up and east.

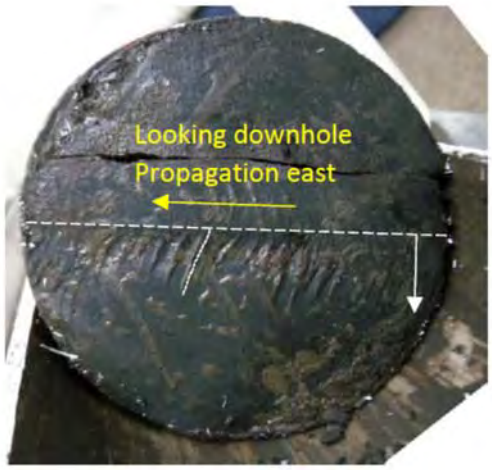

Figure 12. Example of twist hackles with anomalous orientation looking downhole. Hackles suggest downward propagation. Twist-hackle asymmetry suggests overall propagation to east (left in photo).

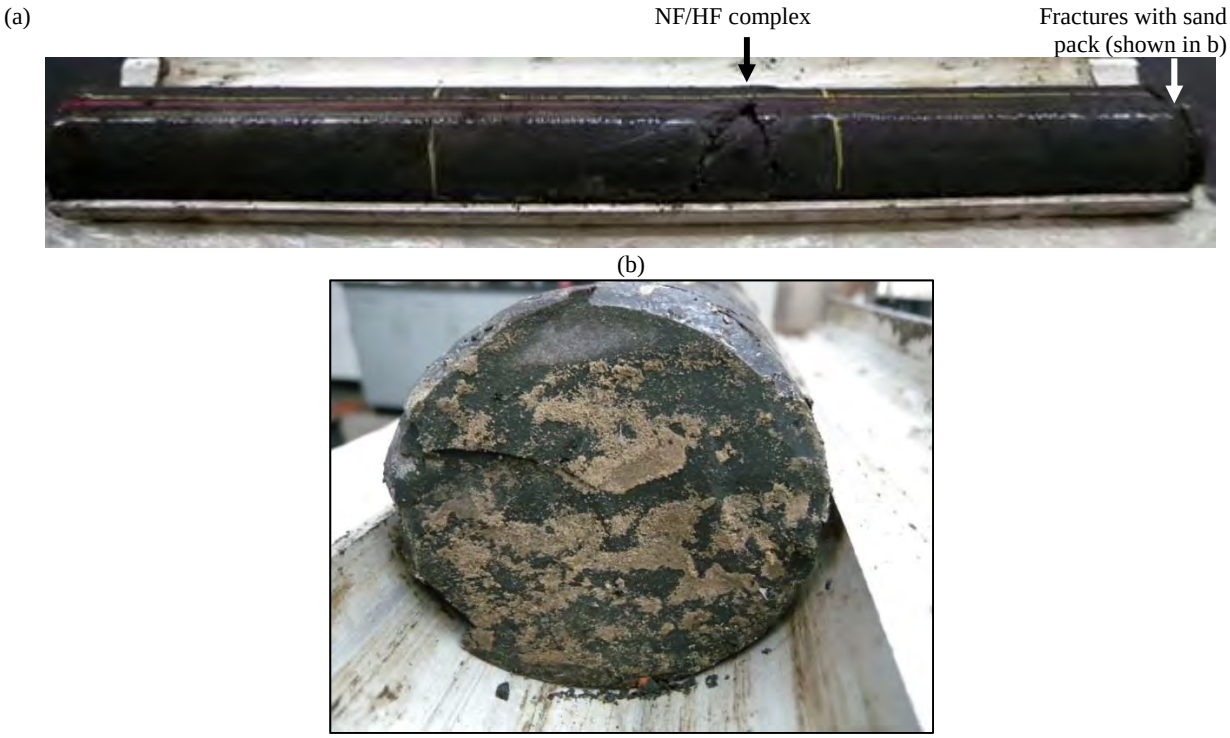

Figure 13. Sand in hydraulic fracture in Upper Wolfcamp. (a) The 3-ft section of core with location of sand pack figured in b, at base of section, where two HFs are in close proximity—termed a *doublet*. Slightly uphole is complex in which hydraulic fracture interacts with Set 2 natural fracture. b) Face of fracture with sand pack, looking uphole.

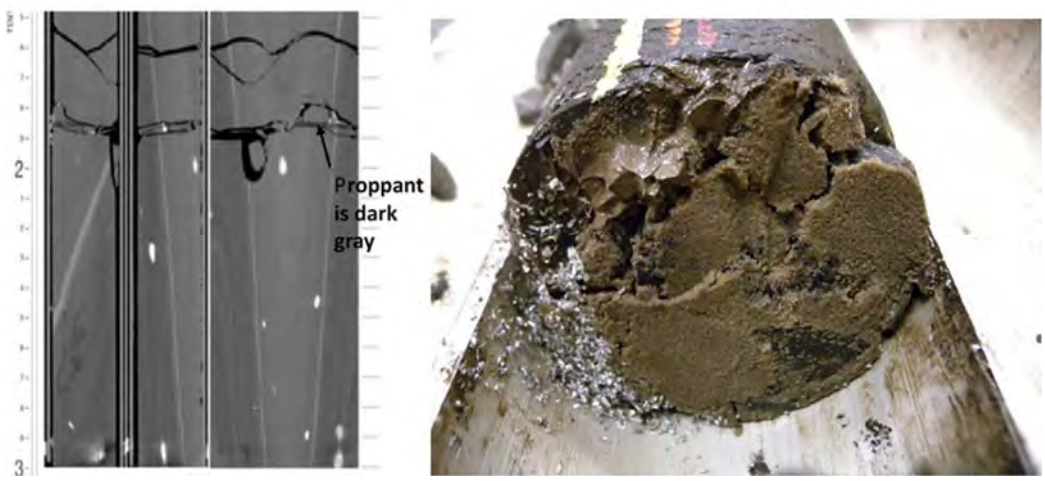

Figure 14. Sand pack in complex hydraulic fracture. (a) CT scan of fracture; proppant dark-gray. (b) Sand pack viewed uphole with core piece below fracture removed. Sand since removed for analysis. Hydraulic fractures at this location have complex geometry possibly favoring trapping of sand pack. The fracture complex is approximately 1 cm wide.

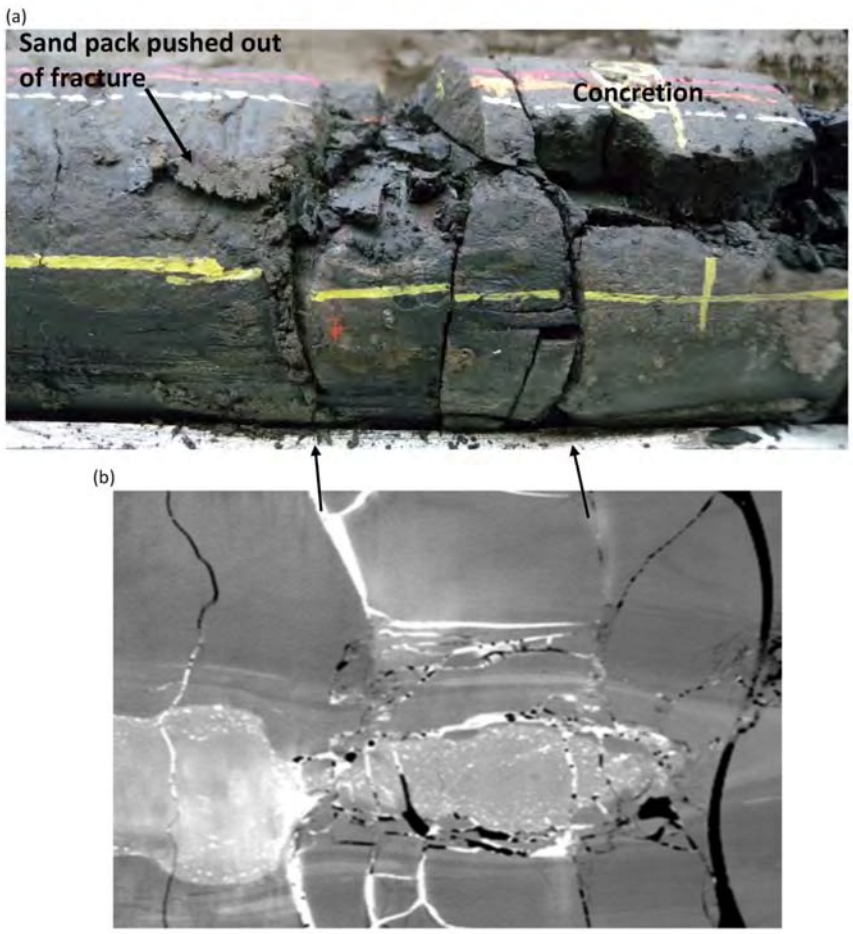

Figure 15. Sand pack in complex hydraulic fracture adjacent to a concretion. (a) Sand on outer surface of core with multiple breaks visible. (b) CT circumferential scan.

In several other locations, there are patches of sand in hydraulic fractures. Some of these occur close to where the main proppant packs are located, whereas others occur away from the packs. In two cases the sand patches coincide with an apparent interaction between a hydraulic fracture and a natural fracture.

Hydraulic fractures reactivating weak planes, such as bedding or natural fractures

Breaks occur along some of the natural fractures and bedding planes, although the reason they are broken (reactivated) is not easy to determine. The mechanism for reactivation could be hydraulic fracturing, drilling, core-retrieval stress, or core handling. For planes reactivated during hydraulic fracturing, possible indicators include:

(1) Bedding-plane breaks connected to a hydraulic fracture (hard linked) (Fig. 16). These are smooth and planar when compared with other bed-parallel breaks, which are stepped and rough. Nonconnected, bed-parallel fractures could open as a result of a pressure front associated with hydraulic fracturing, and in this case would not be hard linked.

(2) Hard-linked, reactivated breaks should have some proppant in them.

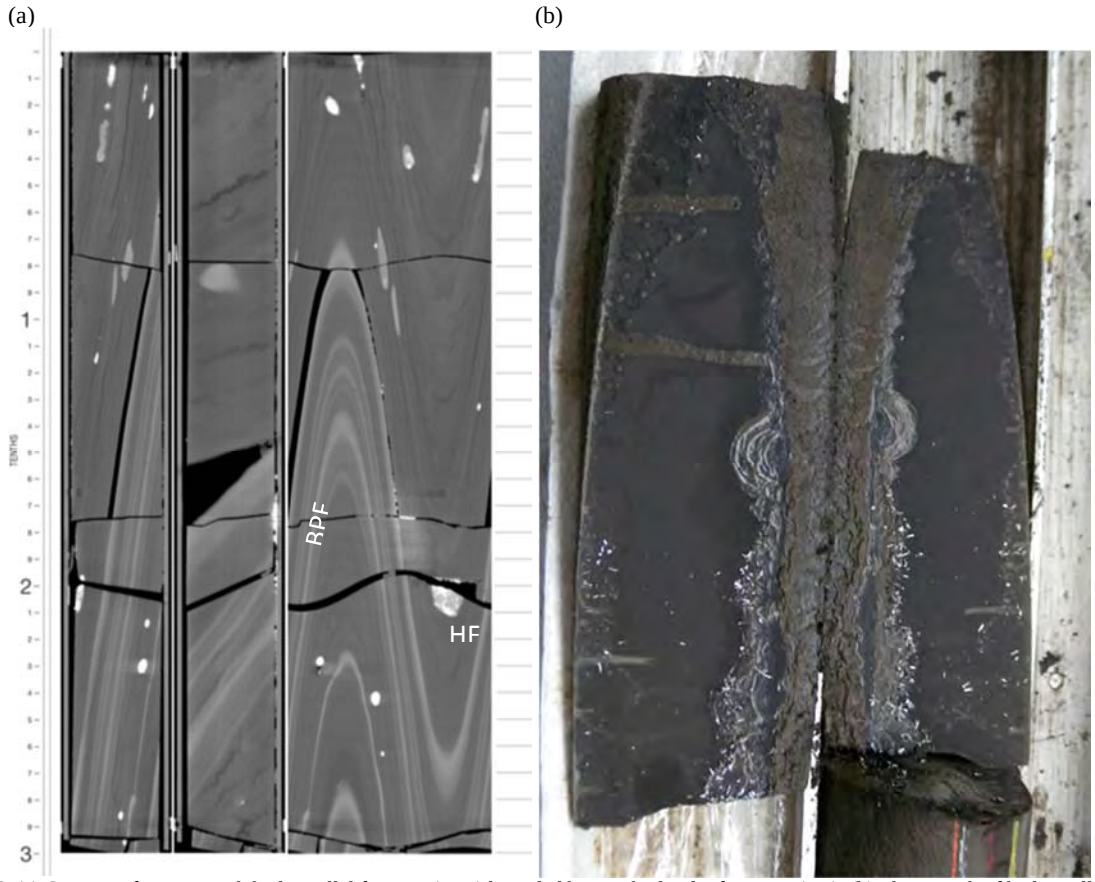

Figure 16. (a) CT scan of section with bed-parallel fracture (BPF) bounded by two hydraulic fractures (HF). (b) Photograph of bed-parallel fracture surfaces, which are smooth and planar. Drilling mud has partly invaded at margins.

Drilling-induced fractures (from drilling the slant well)

Drilling-induced fractures are mostly at a high angle to the well bore and parallel to S_{Hmax}, as are hydraulic fractures. In horizontal or slant wells, drilling-induced fractures can be confined to the core top. In other cases in which the weight-on-bit has increased significantly, breaks can occur along the bedding, with petal shapes extending outward to the core margin (Fig. 17a). Induced fractures commonly have indications of breakage points within the core (e.g., core-rimming plumose markings, and sharp points at the core margin), and they tend to be approximately core symmetric, curviplanar (saddle shaped) (Fig. 17b), or irregular. Surface markings can form, no matter the mechanism. In natural and hydraulic fractures, the markings would have no relation to core margins, barring coincidence. In drilling-induced and core-handling fractures, plumose markings may emanate from a point source within the core. Some proppant grains may also be present, having been brought in with the drilling mud, but proppant will not be present as a sand pack. Drilling can also cause natural fractures or other weak surfaces to break. Differentiating these from reactivation caused by hydraulic fracturing is difficult.

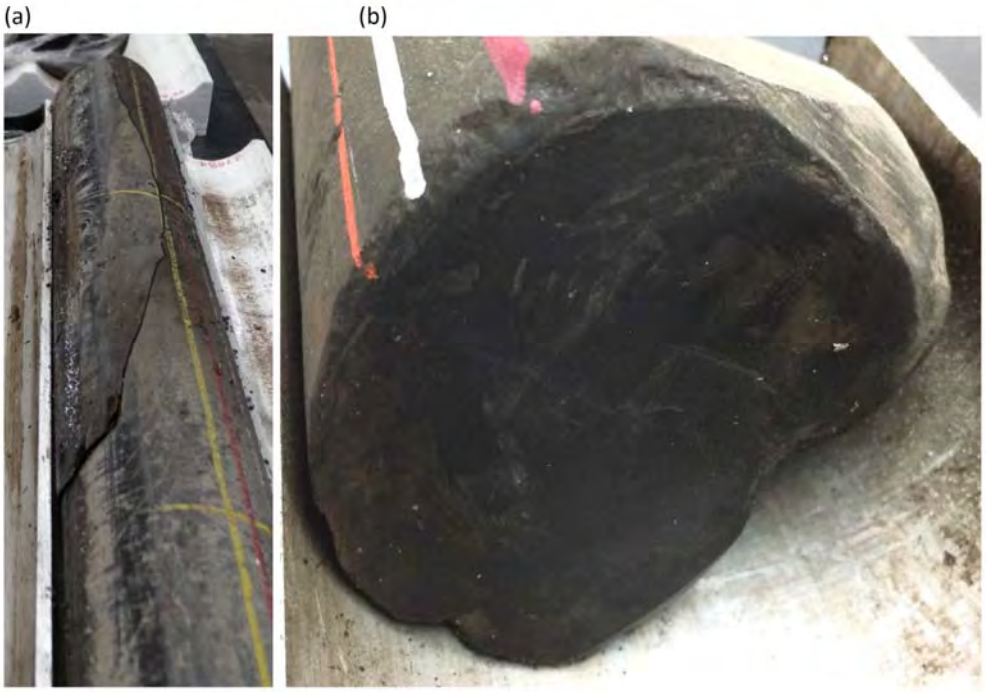

Figure 17. Drilling-induced fractures. (a) Petal centerline shape, viewed looking downhole. (b) Irregular, saddle-shaped fracture.

Core recovery and handling

Core recovery causes vertical-stress release, commonly creating breaks parallel to bedding in vertical cores. In this slant well, few examples occur, and where they do occur, it is commonly at the core margin close to another break. Breaks can also occur during core recovery as the core is retrieved around the bend at the well heel, damage most likely mitigated by the aluminum tube. Sharp points on the fracture face are commonly produced in core during flexural breaking, and in rotary-drilled sidewall plugs they can be used to identify plug orientation (Laubach and Doherty, 1999). Here they are an indicator of breakage after the core has been acquired (Fig. 18).

Figure 18. Likely core recovery fracture with an irregular surface and sharp point (P) suggesting break initiated within core.

Damage can also occur during sawing into sections, transportation, and other handling up to the point of CT-scan acquisition. In these cases, surfaces are rough and fresh, although some drilling mud is generally present (Fig. 19a). These fractures are present in the CT scan; new fractures created as a result of handling/desiccation after CT-scan acquisition are not present in the CT scan. These surfaces are fresh breaks and have no drilling mud (Fig. 19b).

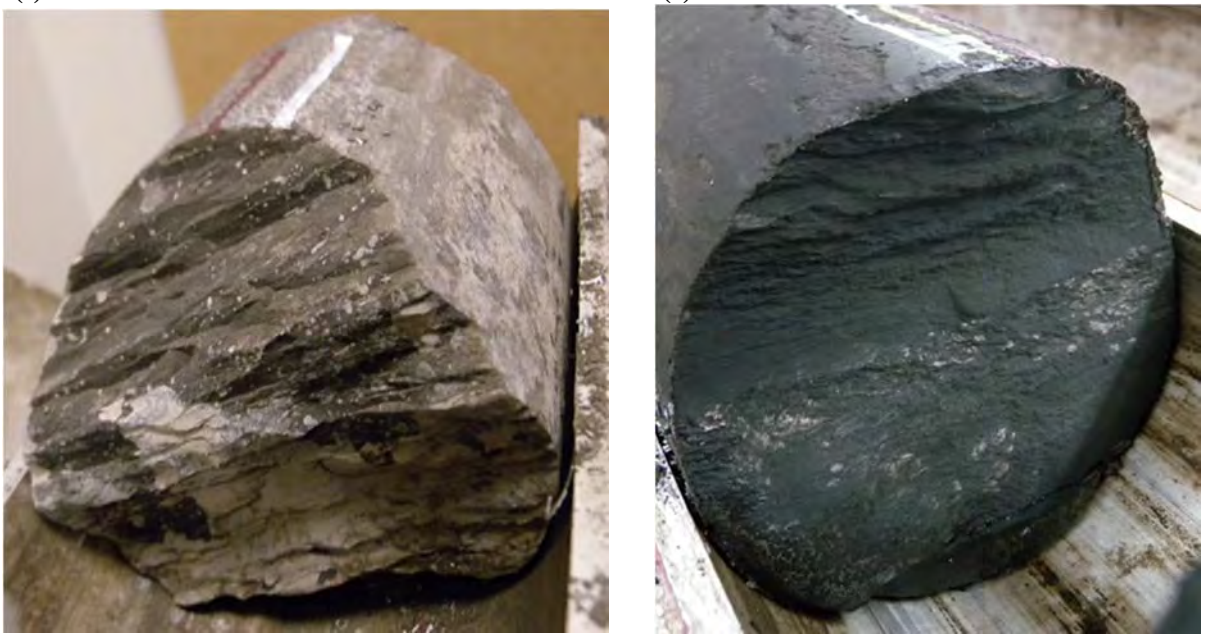

Figure 19. (a) Likely core-handling fracture. Irregular surface with some drilling-mud splatters. (b) Post-CT-scan break. Irregular with rough surface and no drilling mud inside.

Discussion

Systematic description of the 6TW slant cores revealed hydraulic fractures, natural fractures, drilling-induced fractures, and core-handling breaks, and criteria developed for distinguishing these potentially have wider application to other similar datasets. Raterman et al. (2017) observed hydraulic-fracture doublets and triplets in their Eagle Ford study and interpreted them as being the result of HF branching at mechanical interfaces. We see similar features (Fig. 10), and the slant core also captured some branch points, although the reason branching occurs is not clear. No consistent relationship with interfaces of mechanically different layers occurs, for example, and many examples of single planar HFs do not branch at such interfaces.

If the location of the hydraulically fractured wells relative to the slant well is known, the direction of propagation should be predictable and can be compared with observations. For the Upper Wolfcamp, because the hydraulically fractured well (6U) crosses the slant well and lies to the east of it, Cores 1, 2, and part of 3 are above the 6U well. In these cores, hydraulic fractures should propagate upward and to the west, whereas the lower part of 3 and Core 4 are below the 6U, and fractures should propagate downward, although still to the west. In the Middle Wolfcamp, hydraulic fractures would have propagated up from the 6M toward the east. Although some observations are consistent with these predicted propagation directions we observed some anomalies. Surface markings on fractures in outcrop (e.g., Cobain et al., 2015) show that both upward and downward propagation directions can occur in close proximity within a single fracture plane (Fig. 20). Our observations in the slant core may come from both upper and lower twist-hackle (fringe) zones. The lateral propagation direction, however, should be determinable from asymmetry of twist hackles (c.f. Fig. 20) or from branching. A possible explanation for anomalous, inferred propagation directions is that the premise that fractures always propagate away from the well bore may not be correct. If some fractures initiated away from the well bore, then they may propagate laterally in opposing directions at the same time. A further, systematic analysis of all propagation-direction indicators in the slant core might illuminate the apparent anomalies in inferred propagation direction.

It is well established that geologic discontinuities, including natural fractures, can be reactivated during hydraulic-fracture treatments, even when sealed with mineral cements (e.g., Dahi-Taleghani and Olson, 2011; Gale et al., 2014). Laboratory experiments in which a propagating crack interacts with a cement-filled natural fracture reveal the controlling factors that determine whether the hydraulic fracture arrests, diverts, or terminates against the natural fracture are the angle of approach and the thickness of the natural fracture (Lee et al., 2015). In this study we noted that whereas some of the natural fractures are reactivated, many remain intact (Fig. 4b). The natural fractures in Set 1 are favorably oriented for reactivation and are mostly less than 1 mm wide, yet commonly they are not reactivated. At the scale of a fracture stimulation, fracture patterns and in situ stress can be highly variable, even though the broad tectonic pattern may be consistent over hundreds of miles. Site-specific evaluation of natural fractures and in situ stress is therefore necessary. The many aspects of interest include the bifurcation and clustering of hydraulic fractures, and possible reactivation of preexisting discontinuities in the host rock. We envisage further analysis of this dataset yielding more information about growth of the hydraulic-fracture network. This information can then be used to better plan future wells and potentially provide additional information about the stimulated reservoir volume.

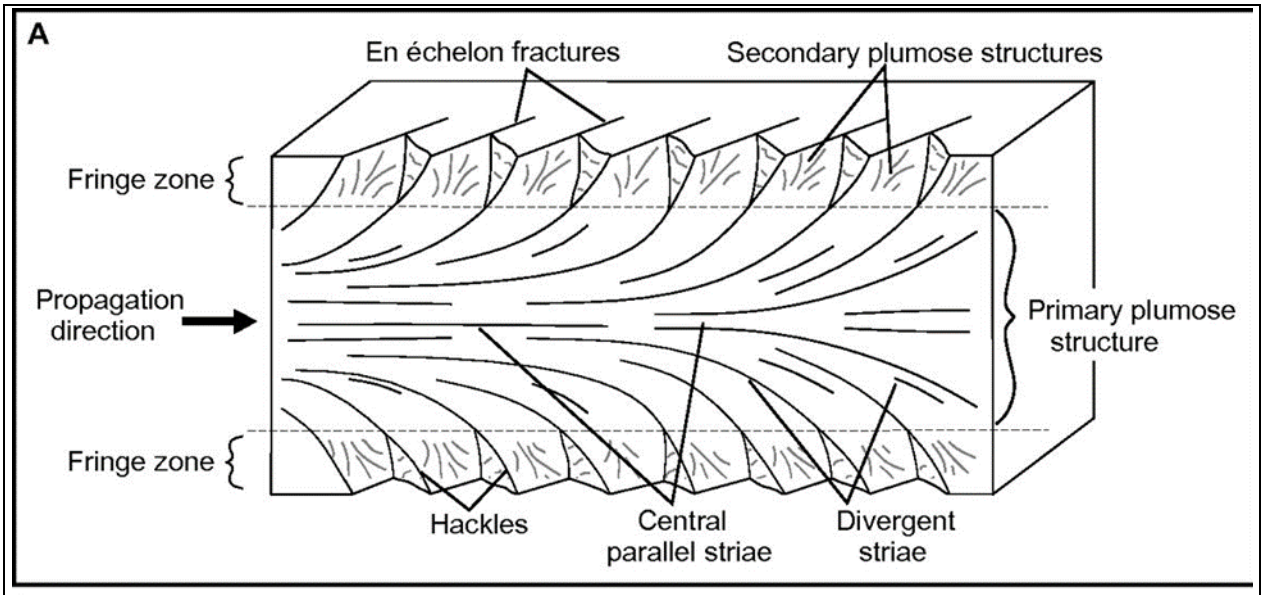

Figure 20. Diagram of plumose structure on a joint surface (from Cobain et al. (2015), their figure 6A). Note local direction of propagation indicated by twist hackles is up at the top and down at the base.

Conclusions

In the 6TW well, over 700 fractures, comprising hydraulic fractures, calcite-filled natural fractures, drilling-induced fractures, and core-handling breaks in approximately 600 ft of slant cores, were described, although fractures are not evenly distributed along the length of the cores. Hydraulic fractures may be distinguished from drilling-induced fractures on the basis of morphology and surface markings. Natural fractures contain calcite cement, and they are mostly intact. Only two natural fractures were open in the subsurface prior to stimulation; they are now parted, but euhedral calcite crystals are present on the faces. Only a few bedding-parallel breaks were observed, and there is no beef.

The potential benefits of this project include verification of theoretical ideas/models of hydraulic-fracture growth of the well in question, as well as insights into the complexity (or otherwise) of the hydraulic-fracture system. Moreover, opportunities for a better understanding of microseismicity and/or aseismic fracture growth through comparison of microseismic event locations versus hydraulic-fracture paths abound.

Acknowledgments

Laredo Petroleum Company provided data and informative discussion. The work was funded as a subcontract under the Gas Technology Institute's (GTI) NETL contract DE-FE0024292. The project was coordinated by GTI, with Jordan Ciezobka providing project management, practical help with core-handling method selection, and discussion of results. Thanks to Seth Busetti (ConocoPhillips) and Helen Farrell (Twenty Sixth Street Consulting LLC) for sharing their fracture orientation data and for helpful discussions on fracture interpretation. CoreLabs provided CT scans of the slant core, which were invaluable as a tool for interpretation. CoreLabs staff were instrumental in the successful execution of this core description, handling all logistics of cutting open the tubes, cleaning the exterior surface, and marking, laying out, and repackaging the core. The GTI HFTS Consortium also provided helpful input to interpretation. Publication authorized by the Director, Bureau of Economic Geology, The University of Texas at Austin.

References

Branagan, P. T., Peterson, R. E., Warpinski, N. R., and Wright, T. B., 1996. Characterization of a remotely intersected set of hydraulic fractures: results of intersection well No. 1-B GRI/DOE Multi-Site Project, *in* Society of Petroleum Engineers, SPE Annual Technical Conference & Exhibition, Denver, October 6–9, SPE Paper No. 36452.

Cobain, S. L., Peakall, J., and Hodgson, D. M., 2015, Indicators of propagation direction and relative depth in clastic injectites: implications for laminar versus turbulent flow processes: GSA Bulletin, v. 127, p. 1816–1830; doi: 10.1130/B31209.1.

Cobbold, P. R., Zanella, A., Rodrigues, N., and Løseth, H., 2013, Bedding-parallel fibrous veins (beef and cone-in-cone): worldwide occurrence and possible significance in terms of fluid overpressure, hydrocarbon generation and mineralization: Marine and Petroleum Geology, v. 55, p. 250–261, doi:10.1016/j.marpetgeo.2013.01.010.

Courtier, J., Ciezobka, J., 2018 (this volume), Hydraulic fracture test site—project overview and summary of results: URTeC Paper No. 2937168.

Dahi-Taleghani, A., and Olson, J. E., 2011, Numerical modeling of multistranded-hydraulic-fracture propagation: Accounting for the interaction between induced and natural fractures: SPE Journal, v. 16, p. 575–581.

Elliott, S. J., et al., 2018 (this volume), Analysis and distribution of proppant recovered from fracture faces in the HFTS Slant Core drilled through a stimulated reservoir: URTeC Paper No. 2902629, 10 p.

Fast, R. E., Murer, A. S., and Timmer, R. S., 1994, Description and analysis of cored hydraulic fractures—Lost Hills field, Kern County, California, *in* Society of Petroleum Engineers, SPE Production and Facilities, p. 107–114. SPE Paper No. 25843.

Fisher, K., and Warpinski, N., 2012, Hydraulic fracture height growth: real data, *in* Society of Petroleum Engineers, SPE Production and Operations, SPE Paper No. 145949.

Gale, J. F. W., Laubach, S. E., Olson, J. E., Eichhubl, P., and Fall, A., 2014, Natural fractures in shale: a review and new observations: AAPG Bulletin, v. 98, p. 2165–2216.

Ortega, O. J., Marrett, R. A., and Laubach, S. E., 2006, A scale-independent approach to fracture intensity and average spacing measurement: AAPG Bulletin, v. 90, p. 193–208.

Laubach, S. E., and Doherty, E., 1999, Oriented drilled sidewall cores for natural fracture evaluation, *in* Society of Petroleum Engineers, Formation Evaluation and Reservoir Geology, SPE Paper No. 56801, p. 793–800.

Lee, H. P., Olson, J. E., Holder, J., Gale, J. F. W., and Myers, R. D., 2015, The interaction of propagating opening mode fractures with preexisting discontinuities in shale: Journal of Geophysical Research: Solid Earth, v. 120, p. 169–181.

Lund Snee, J.-E., and Zoback, M. D., 2016, State of stress in Texas: implications for induced seismicity: Geophysical Research Letters, v. 43, p. 10208–10214, doi:10.1002/2016GL070974.

Raterman, K. T., Farrell, H. E., Mora, O. S., Janssen, A. L., Gomez, G. A., Busetti, S., McEwen, J., Davidson, M., Friehauf, K., Rutherford, J., Reid, R., Jin, G., Roy, B., and Warren, M., 2017, Sampling a stimulated rock volume: an Eagle Ford example: Unconventional Resources Technology Conference, Austin, July 24–26, URTeC Paper No. 2670034.

Warpinski, N. R., Lorenz, J. C., Branagan, P. T., Myal, F. R. and Gall, B. L., 1993, Examination of a cored hydraulic fracture in a deep gas well: Society of Petroleum Engineers, SPE Production & Facilities, August, p. 150–158. SPE Paper No. 22876.